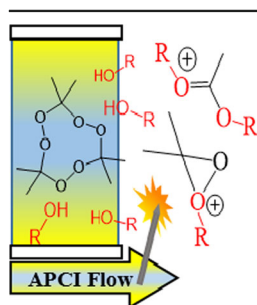


RESEARCH ARTICLE

Reactions of Organic Peroxides with Alcohols in Atmospheric Pressure Chemical Ionization—the Pitfalls of Quantifying Triacetone Triperoxide (TATP)

Kevin Colizza, Alexander Yevdokimov, Lindsay McLennan, James L. Smith, Jimmie C. Oxley

Department of Chemistry, University of Rhode Island, 140 Flagg Rd., Kingston, RI 02881, USA



Abstract. Over the last several decades, mass spectrometry has become one of the principle methods for compound identification and quantification. While for analytical purposes, fragments which are not fully characterized in terms of origin and intensity as a function of experimental conditions have been used, understanding the nature of those species is very important. Herein we discuss such issues relative to triacetone triperoxide (TATP) and its frequently observed fragment at m/z 89. This “fragment” has been identified as the gas-phase reaction product of TATP with one or two methanol molecules/ions. Additionally, the origin and conditions of other fragments at m/z 91, 75, and 74 associated with TATP will be addressed. Similar analytical issues associated with other multi-peroxide organic compounds [hexamethylene triperoxide diamine (HMTD), methyl ethyl ketone peroxides (MEKP)] will also be discussed. Solution storage conditions for TATP, HMTD, and tetramethylene diperoxide diamine dialdehyde have been determined.

Keywords: TATP, HMTD, TMDDD, Organic peroxides, Gas-phase reaction with alcohols, Triacetone triperoxide, Hexamethylene triperoxide diamine, Tetramethylene diamine diperoxide dialdehyde

Received: 15 September 2017/Revised: 10 October 2017/Accepted: 11 October 2017/Published Online: 7 November 2017

Introduction

Terrorist incidents and resulting government focus on so-called “homemade” explosives have resulted in a number of researchers examining the organic peroxides. Synthesized triacetone triperoxide (TATP) [1], hexamethylene triperoxide diamine (HMTD) [2], and methyl ethyl ketone peroxides (MEKP) [3] (Figure 1) are the most commonly encountered because of their ease of formation. With attention being on rapid detection and analysis, traditional analytical tools, infrared [4], Raman [4, 5], and X-ray [5] have been applied. However, screening usually employs ion mobility mass spectrometry (IMS) [6–8]. Spectroscopy, which offers no possibility of separation from interferences, has reported limits of detection (LOD) ranging between 1 [9] and 5 ppm [10] in standoff mode. IMS, which has some ability to separate interferences, has a

reported LOD of 23.3 ng for TATP and 0.2 ng for HMTD [8]. For unequivocal identification and quantification, some type of separation is essential prior to detection.

Volatile organic compounds have traditionally relied on separation by gas chromatography (GC) coupled to either a mass spectrometer (MS) [11–15] or electron capture detector (ECD) [13, 16]. In one of the earliest reports of TATP detection in a criminal case study, both GC/MS electron ionization (EI) and chemicals ionization (CI) techniques were used [17]. Since that time, the number of GC/MS applications for TATP and HMTD have grown exponentially; today it is one of the prominent techniques for their detection. The reported LODs for TATP in a condensed phase range between 0.05 and 2 ng [18], depending on the mode of ionization and type of mass spectrometer used; even lower LODs (<0.1 ng) are recorded for headspace analysis [19]. Low nanogram levels were reported by DART-time-of-flight-MS [20] for HMTD analysis. The major drawback using GC is the potential for thermal degradation of explosives in the inlet or ion source. For this reason, liquid chromatography mass spectrometry (LC/MS) is becoming a predominant technique for unequivocal structural elucidation and quantification of most organic molecules. The

Electronic supplementary material The online version of this article (<https://doi.org/10.1007/s13361-017-1836-3>) contains supplementary material, which is available to authorized users.

Correspondence to: Jimmie Oxley; e-mail: joxley@chm.uri.edu

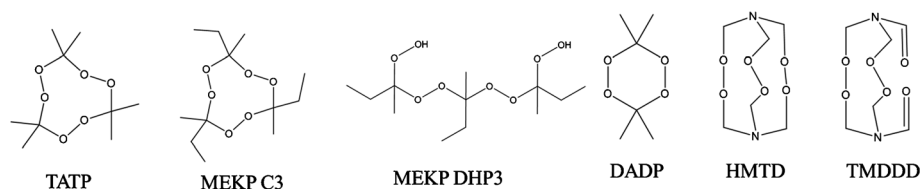


Figure 1. Structures of peroxides analyzed

benefits over GC include room temperature sample introduction, availability of soft ionization techniques, and high resolution accurate mass capability [21, 22]. Selected MS interface methods with monitored ions and LODs are presented in Table 1.

Much of the reported research utilizing LC/MS was performed on nominal mass instruments, making some assignments and fragment origins questionable [25]. For example, though many researchers identify or quantify TATP using m/z 89 [6, 7, 21, 29], exact mass MS shows this fragment contains four carbons, which cannot readily be explained from the structure of TATP (Figure 1). Our work investigates the origin of that fragment and addresses chromatographic and mass spectrometric parameters (e.g., solvents [35], temperatures, gas flows, and voltage differentials) that can affect ion production.

Materials and Methods

Chemicals and Reagents

Caution: The organic peroxides mentioned below are powerful explosives. Take all necessary precautions when working with these compounds.

Water, acetonitrile, methanol, 2-propanol (all Optima HPLC grade), ammonium acetate (NH_4OAc), sodium acetate,

lithium acetate, n-butanol (all HPLC grade), n-propanol (sequencing grade), tert-butanol, methyl ethyl ketone (MEK), and acetone (ACS grade) were purchased from Fisher Chemical (Fair Lawn, NJ, USA). Stable isotope labeled material was purchased from Cambridge Isotope Labs (Cambridge, MA, USA). Hexamethylenetetramine (hexamine) was purchased from Acros Organics (Morris Plains, NJ, USA). Hydrogen peroxide (HP, 50%) was purchased from Univar (Redmond, WA, USA). All mobile phase used for chromatography consisted of aqueous 10 mM NH_4OAc prepared at neutral pH with methanol (MeOH) as the organic modifier unless otherwise stated.

TATP, DADP, TMDDD, and MEKP Synthesis

Triacetone triperoxide (TATP) and diacetone diperoxide (DADP) were synthesized according to literature methods [13]. TATP was purified by recrystallizing once with 80/20 (w/w) MeOH/ H_2O and then with pentane [melting point (mp) 94–96 °C]. Deuterated TATP (d_{18} -TATP) was synthesized as above [13] using d_6 -acetone. DADP was recrystallized in hot methanol (mp: 131–133 °C).

For hexamethylene triperoxide diamine (HMTD) synthesis, a round-bottom flask equipped with magnetic stir bar was used to dissolve hexamine (2.43 g, 17.3 mmol) in 50% hydrogen peroxide (9.88 g, 145 mmol) and chilled in an ice bath. Anhydrous citric acid (3.61 g, 18.9 mmol) was added in small portions so that the temperature did not exceed 10 °C. The

Table 1. MS interface methods with reported LOD for peroxide explosives

Peroxide	LOD (ng)	Monitored ions (m/z)	Ionization Mode	Ref
TATP	62.5	[245], 215, 81	APCI	[23]
	20	[229]	EESI	[24]
	15	[240], 242, 224, 223, 210	DBDI	[25]
	10	[245], 240, 223, 215, 91, 74	DESI	[26]
	25	252, 240, 194, 107, 102, 91, [89], 90, 75	APCI	[21]
	1-50	[240], 245, 223	DESI	[22]
	0.8-148	[223], 240, 132, 91, 74	APCI	[27]
	0.88	240.1441, 89.0597	APCI	[28]
	1	89.0597	APCI	[29]
	0.1	348.1869	APCI	[30]
HMTD	3	[229], 209, 191, 145, 104	APCI	[31]
	1	[231], 247, 209	DESI	[26]
	10,000	[224], 177, 207, 209	APCI	[32]
	0.08-12	[118], 207, 191, 147, 72, 58	APCI	[27]
	-	[209], 224, 207, 179, 145, 88	DART	[33]
	0.43	[207.0975], 209.0768, 179.0666, 145.0606	APCI	[28]
	2.5	207.0976	APCI	[29]
	1	[209], 207, 179, 106, 90, 62	APCI	[34]
	0.2-0.5	207.0615, 177.0861	APCI	[30]

LOD = limit of detection, $[m/z]$ = most abundant observed ion, APCI = atmospheric pressure chemical ionization, ESI = electrospray ionization, DESI = desorption electrospray ionization, DART = direct analysis real time, DBDI = dielectric barrier discharge ionization, EESI = extractive electrospray ionization

reaction mixture was left in the ice bath and stirred for 15–18 h. Product was collected by vacuum filtration, washed with deionized water and room temperature methanol, and allowed to dry. This HMTD was used to produce tetramethylene diperoxide diamine dialdehyde (TMDDD), which was synthesized according to Wierzbicki et al. [36]. The crude product (mp: 156–157 °C) was used for all TMDDD testing.

Methyl ethyl ketone peroxides were synthesized by a modified literature method [37]. In a test tube containing a micro stir bar, hydrogen peroxide (50-wt%, 1.4 mL) was mixed with methyl ethyl ketone (0.82 mL, 9.49 mmol). The solution was chilled in an ice bath and concentrated H₂SO₄ (0.5 mL, 9.38 mmol) was added slowly so that the temperature did not exceed 20 °C. Stirring continued for 15–18 h before the solution was extracted with pentane, washed with saturated ammonium sulfate (3 × 3 mL), deionized water (3 × 3 mL), and dried with sodium sulfate. The product was stored as a solution in pentane and was pipetted into tared vials for immediate dilution with MeOH to desired concentrations.

Instrumentation

Using a Thermo Electron LTQ Orbitrap XL or Exactive mass spectrometer equipped with an atmospheric pressure chemical ionization (APCI) interface, ions were generated and introduced into the ion transfer tube set between 180 and 275 °C (depending on the experimental conditions being tested). All work was performed using positive ion mode. Tune conditions for APCI infusion experiments were varied depending on the parameters being tested: discharge current, 2500–6000 μ A; N₂ sheath gas, 8–50 arbitrary units (AU); N₂ auxiliary gas, 5–40 AU; vaporizer temperature 180–350 °C; ion transfer tube, 14 V; tube lens, 35–70 V; and skimmer offset (Exactive), 0 V. Minor voltage changes were made at times to improve signal intensity for some compounds. Mass resolution was set to 30,000 (LTQ Orbitrap) and 50,000 (Exactive) for all experiments. Solvent delivery was performed using either Thermo infusion syringe pumps or Thermo Electron Accela quaternary pumps. A CTC Analytics HTS PAL autosampler injected directly from either amber glass LC vials with PTFE septa (Agilent Technologies) or polypropylene, 1 mL 96-well plates with pre-slit silicone plate covers (Analytical Sales and Service). Data collection and analysis was performed with Thermo Xcalibur software ver. 2.2, SP 1.48. All data collected within this work is APCI full scan MS unless otherwise noted. Chromatographic traces are all extracted ion chromatograms (XIC) with a mass window of 15 ppm of the expected exact mass. Note: All masses reported below are exact mass values within ± 15 ppm for species less than 130 m/z and ± 7.5 ppm for species over m/z 130.

TATP Analysis

The mass spectrometry gas flows and temperature were originally optimized using a constant flow of 50% 10 mM NH₄OAc in pump channel B and 50% MeOH in channel A at 230 μ L/min flow and directly infusing 20 μ L/min TATP standard (20

μ g/mL/90.1 μ M in MeOH) into the flow. Monitoring the [M+NH₄]⁺ ion at m/z 240.1442, the vaporizer temperature was set to 250 °C, with the sheath gas at 40 AU and auxiliary gas at 20 AU. Using this optimized system, 40 μ L sample volumes of TATP in 50/50 ACN/water were injected into a LC flow of 250 μ L/min with 5% MeOH (channel A) and 95% aqueous 10 mM NH₄OAc (channel B) for introduction onto a Thermo Syncronis C18 column (2.1 × 50 mm, 5 μ m). Initial conditions were held for 1.5 min before a linear ramp to 35% A/65% B over 1.5 min followed immediately by a linear ramp to 95%A/5% B over the next min. This concentration was held for 2 min before a 30 s transition to initial conditions with a hold of 1.5 min. As an internal standard (IS), d₁₈-TATP at 10 μ g/mL (41.7 μ M) in ACN was added 1:1 to aqueous TATP samples with a final concentration of 5000 ng/mL (20.8 μ M). XIC were integrated using the Genesis peak detection algorithm in Thermo Xcalibur Quan Browser. Linear dynamic range comparing concentration to peak area response ratio, relative to the IS, extended from 25 ng/mL (112.6 nM) to 20000 ng/mL (90.1 μ M) using 10 points and 1/x weighting of the calibration curve. Identical procedures were followed for the calibration curve of DADP (discussed later). Stability determination for TATP did not use an IS and calibration was determined by peak area response versus concentration (external calibration). Linear range and curve conditions were the same as above. All dilutions were made in 50/50 ACN/water. Stability was determined by comparing quality control (QC) samples made on day one to freshly prepared standards made on the day of stability determination.

TATP Volatility

Volatility of TATP was interrogated by two methods. The first involved incubating aqueous TATP at 37 °C in 1.5 mL Eppendorf tubes both open and closed. For this analysis, 995 μ L of water was brought to 37 °C before addition of 5 μ L of 20 mM TATP in ACN (final concentration 100 μ M) to initiate the study (time 0). At time 0, 15, 30, 45 and 60 min, 100 μ L aliquots were removed and placed in 100 μ L of ACN containing internal standard. Analyses were performed in duplicate and average values are displayed with RSD values less than 0.5%. The second method involved placing 100 mg of TATP powder in two separate 1L vessels (screw top) and two separate 500 mL vessels (screw top). Each vessel was covered with aluminum foil, capped, and allowed to remain at room temperature (~ 20 °C) for ~ 4 h. For each vessel, three labeled GC vials were filled with 500 μ L of 50/50 ACN/water and capped with PTFE septa seals. At 4 h, the cap was removed from the first vessel; a 2.5 mL, gas-tight hypodermic syringe penetrated the foil to withdraw 2.5 mL of vapor, and the cap was immediately replaced. The vapor was transferred into the GC vial ensuring the needle tip was well under the liquid while the plunger was slowly depressed and the vial gently swirled. This was repeated three times for each vessel before sample solutions were injected onto the HPLC/MS system

described above (without IS). Samples were injected in duplicate; average TATP vapor concentration is reported.

HMTD/TMDDD Analysis

Stability determination of HMTD ($[M+H]^+$ ion of m/z 209.0768) and TMDDD ($[M+NH_4]^+$ ion of m/z 224.0877) were performed by the same method used for TATP to keep analysis consistent for these three compounds. All dilutions were made in 50/50 ACN/water. The HMTD 9-point external calibration curve was linear from 50 ng/mL (240 nM) to 20000 ng/mL (96.2 μ M). TMDDD was linear over a 10-point external calibration from 25 ng/mL (121 nM) to 20,000 ng/mL (97.1 μ M). Stability was determined by comparing QC samples made on d 1 to freshly prepared standards made on the day of stability determination.

MEKP Analysis

Since the MEKP's lacked any true "standard", stability determinations or quantitative analysis of any specific species was not possible. Purification of these compounds, particularly the cyclic trimer (MEKP C3), was attempted using a CombiFlash Rf+ PurIon (Teledyne Isco, Lincoln, NE, USA) system with C18 cartridges. HPLC methods developed for this system are as follows. A 25 μ L sample containing an estimated 20 μ g/mL (by weight) of total MEKP was injected onto the Synchronis C18 column into 250 μ L/min flow of mobile phase 65% A/35% B. Initial conditions were held for 1 min followed by a linear ramp to 80% A/20% B over 3 min and a 6-min isocratic hold. Conditions were then changed to 98% A/2% B over 30 s and held for 1.5 min before dropping to initial conditions over 30 s with a 2-min hold. Using this method, we were able to achieve baseline separation of what we believe to be the MEKP C3 ($[M+NH_4]^+$ m/z 282.1911) from other linear peroxides.

Isotope Incorporation Studies

To examine the origin of certain products/fragments observed in the LC/MS experiments, isotope incorporation studies were performed as follows. Hydrogen/deuterium exchange (HDX) began with concentrated (20 μ g/mL), 0.5 mL samples of TATP and d_{18} -TATP prepared in deuterium labeled methanol/water (CD_3OD/D_2O) and unlabeled ($MeOH/H_2O$) solvents, respectively. An ammonium source was provided by the addition of 5 μ L of 500 mM NH_4OAc . Solutions were individually infused at 20 μ L/min. Two samples containing an estimated 30 μ g/mL of total MEKP and 20 μ g/mL of both TATP and d_{18} -TATP were produced from highly concentrated standards prepared in MeOH. These samples were briefly placed under a light stream of N_2 gas to evaporate the solvents but prevent significant evaporation of TATP. One sample was reconstituted in 100 μ L of MeOH and 20 μ L of water before infusion onto the optimized APCI-MS conditions for in-source fragment production (discussed later). Once this sample was successfully

observed, the second sample was reconstituted in 100 μ L of $Me^{18}OH$ and 20 μ L of water and infused.

Alcohol Incorporation and Infusion Experiments

A 25 μ L sample containing an estimated 20 μ g/mL of total MEKP and 10 μ g/mL of both TATP and d_{18} -TATP was injected onto the LC/MS system developed for MEKP (above). Mobile phase transition from MeOH to isopropanol (IPA) or n-propanol (PrOH) required significant change due to the higher solvent strength and column back pressure of the larger alcohols. The same sample (25 μ L) was injected into a mobile phase of 20% PrOH/80% B flowing at 200 μ L/min onto the C18 column. Conditions were held for 1 min followed by a linear ramp to 90% PrOH/20% B over 8 min. This was held for 1 min before ramping to initial conditions over 30 s and holding for 2 min.

Infusion of TATP into the APCI source was performed by two methods. To generally optimize MS voltages, TATP (20 μ g/mL in 90/10 MeOH/10 mM NH_4OAc) was directly infused onto the APCI source at 20 μ L/min. We termed this "direct infusion." To assess the effects of temperature and gas flow, TATP (20 μ g/mL in 90/10 MeOH/10 mM NH_4OAc) was infused at 20 μ L/min into a 230 μ L/min flow of 95% MeOH/5% 10 mM NH_4OAc (total flow was 250 μ L/min, the environment of TATP eluting from a C18 column). This we termed "MP infusion." An additional MP infusion study was performed but using the TATP gradient program (described above). Full scan data were collected from m/z 70 to 500, and the XIC data for TATP $[M+NH_4]^+$ and m/z 89.0597 were exported to Microsoft Excel for data analysis. Additional studies to show incorporation of various alcohols were performed by directly infusing 20 μ g/mL samples of TATP and d_{18} -TATP in 20% 10 mM NH_4OAc /80% alcohol. Alcohols (other than MeOH) tested were ethanol (EtOH), PrOH, n-butanol (BuOH), and tert-butanol (t-BuOH).

Results and Discussion

Stability and Volatility of Analytes

Many unexpected challenges and unusual findings were encountered during the development of LC/MS analysis methods for the peroxide explosives TATP, DADP, HMTD, TMDDD, and MEKP. Samples can be prepared and stored in ACN without issue as long as MeOH is used as the organic mobile phase modifier for reverse phase LC/MS and the compound is not eluting in the void volume. The peroxides described in this work are generally well-retained and free of acetonitrile in the source, which is washed away in the sample plug. However, if ACN is present in the source using either ESI or APCI, the signal will be significantly reduced or almost completely eradicated [35].

Individually synthesized products of TATP, HMTD, and TMDDD were treated separately for stability analysis. While attempts were made to purify HMTD, it always contained a

small amount of TMDDD and vice versa. Solutions of each peroxide were prepared and stored in acetonitrile. Autosampler stability (for the 10,000 and 5000 ng/mL samples), is presented in the [Online Resource](#) for the first reanalysis (d 7) since concentrations were changing rapidly once the container seal was compromised. Samples were run at $N = 2$ (RSD <5%). Calibration curve values were within $\pm 15\%$ of nominal concentrations with R^2 values >0.98 for $1/\times$ or $1/\times^2$ weighted curves. TATP showed $\sim 9\%$ recovery after 7 d storage in the refrigerated autosampler (in a 96-well plate, Table S-1, [Online Resource](#)). This loss of TATP is attributed to its high volatility and the fact that the 96-well mat was no longer sealed; subsequent data supports this conclusion.

The peak shape of HMTD on a C18 column was strongly dependent on the organic concentration in the sample plug. As the organic concentration increased, the peak fronting became severe, with optimal peak shape occurring at low organic content. By placing the samples in 50/50 ACN/water, peak shape and limit of detection for HMTD was compromised to keep sample processing consistent with the previously developed method for TATP analysis. Despite this compromise, HMTD curve and QC data were within acceptable criteria of $\pm 15\%$ accuracy. As ACN evaporated from the 96-well plate, concentration of HMTD and TMDDD increased significantly. Evidence of ACN evaporation was observed by the greatly improved peak shape of the HMTD sample after remaining in the autosampler for 7 d (Table S-1, Figure S-1, [Online Resource](#)). In fact, due to the change in concentration of HMTD or TATP, calibration samples run at the start of an analytical series did not replicate results if re-injected at the end of an analysis that lasted over 3 or 4 h.

TATP concentration was relatively unchanged over 60 d under conditions where the storage vessel was airtight. HMTD degraded $\sim 15\%$ in 40 d at room temperature and about 7% in the refrigerator or freezer in 60 d (Table S-1, [Online Resource](#)). This loss corresponds to a similar increase in TMDDD levels in the HMTD samples. This suggests that in ACN, HMTD oxidizes into TMDDD. QC concentrations were kept intentionally high (10,000 to 1000 ng/mL) compared with the curve limits in order to identify degradation products (if possible) and to quantify the conversion of HMTD to TMDDD or vice versa. Concentrations of TMDDD did not appear to decrease, suggesting that this compound did not decompose under the experimental conditions. Storage in methanol or water was not attempted because of lack of solubility of one or more of the compounds in these solvents.

The vapor pressure of TATP is known to be extremely high for a solid. When aqueous solutions of TATP (concentration 100 μM) were incubated at 37 $^\circ\text{C}$ for 60 min in an open 1.5 mL polypropylene Eppendorf tube, the concentration of TATP dropped $\sim 40\%$ every 15 min. To assure that the compound was not degrading under these conditions, the same experiment was performed simultaneously with the snap-cap lid closed. Figure 2 clearly shows that evaporation, not degradation, is the problem that must be overcome during quantitative analysis. This effect is exaggerated at lower TATP concentration

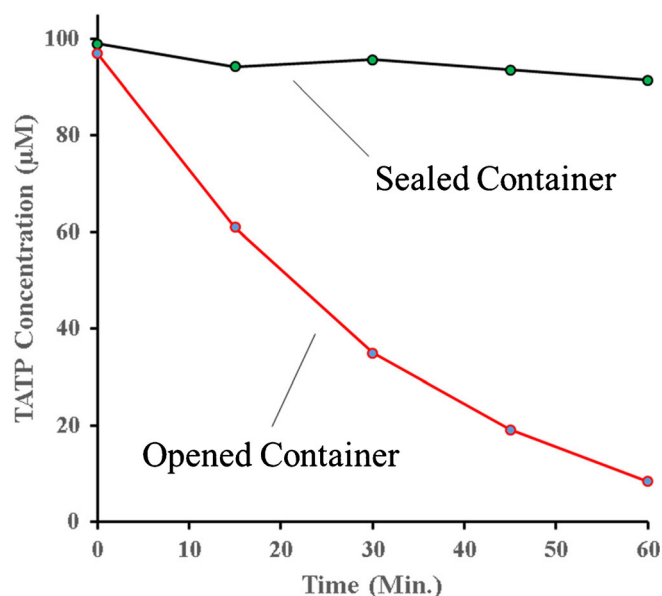


Figure 2. Evaporative loss of TATP (aqueous 100 μM sample) held at 37 $^\circ\text{C}$ in a shaking dry bath

samples ($<10 \mu\text{M}$ kept in closed 1.5 mL Eppendorf tubes) where periodic opening of the tube to remove aliquots resulted in significant evaporative loss up to 3% per tube sampling.

By directly extracting the TATP vapor from the headspace of pure TATP in sealed containers, bubbling that vapor into a solvent system, and quantifying by LC/MS, the concentration of TATP in the headspace was determined to be 376 ng TATP/mL, based on 12 individual trials analyzed in duplicate (Table S-2, [Online Resource](#)). Using the ideal gas law, with a temperature of 20 $^\circ\text{C}$ (293K), the partial pressure of TATP was calculated to be 4.1 ± 0.1 Pa. This is in excellent agreement with the determined partial pressure by headspace GC of 7 Pa in 2005 [16]. It is quite possible that some of the TATP was not fully trapped by the solvent, resulting in a slightly lower partial pressure by this technique.

TATP and MEKP In-Source Fragmentation/Reaction

During the LC optimization of TATP and its fully deuterated analog, d_{18} -TATP (used as an IS), several unexpected “fragment” peaks were observed. Co-eluting with the TATP $[\text{M}+\text{NH}_4]^+$ XIC at m/z 240.1442 was an apparent fragment of m/z 89.0597 corresponding to molecular formula $\text{C}_4\text{H}_6\text{O}_2^+$. Since each TATP ring is comprised of three C_3H_6 units separated by peroxide linkages, making a four-carbon fragment is rather unlikely. When observing the deuterated analog of the $[\text{M}+\text{NH}_4]^+$ ion at m/z 258.2571, the major fragment observed switched from m/z 89.0597 to m/z 95.0974, associated with the molecular formula $\text{C}_4\text{H}_3\text{D}_6\text{O}_2^+$. We speculated that the source of the non-deuterated methyl group was derived from the addition of the solvent methanol into TATP, as we had observed for HMTD [38] and proposed by Rondeau, et al. for dialkyl mono-peroxides [14]. In order to determine the extent of methanol dependence for the m/z 89 signal, TATP was

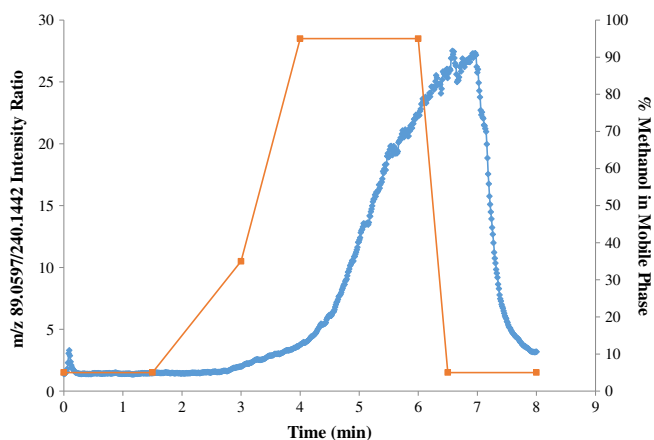


Figure 3. TATP MP infusion into linear gradient of methanol (right) and m/z 89/240 ratio (left)

infused post-column into the normal LC gradient used for TATP analysis. Initially, m/z 240 increased with increasing methanol (as would be expected with increased organic modifier), but that signal quickly leveled off and began to diminish while m/z 89 continued to increase. Although the levels of ammonium were also decreasing, as this was present only in the aqueous phase, the absolute signal of m/z 89 was significantly larger than the loss of m/z 240. To clearly illustrate the

effect of methanol on the m/z 89 fragment, the ratio of m/z 89 to m/z 240 was plotted against time and compared with the methanol concentration of the gradient (Figure 3). There was a significant increase in m/z 89 when ramping the gradient from 5% to 95% methanol. This accounted for some of the previously unexplained variations we had experienced between levels of m/z 89 and m/z 240.

It was noted that under similar LC/MS conditions as used for TATP, each of the MEKP peaks had fragments of m/z 89.0597. This is a reasonable fragment for MEKP since each subunit consists of four carbons. A far more abundant ion at m/z 103.0754, associated with the formula $C_5H_{11}O_2^+$, was also present for each MEKP chromatographic peak. This “fragment” could be explained readily by the incorporation of methanol. To support the hypothesis of methanol incorporation into TATP and MEKP, the mobile phase was changed from methanol to n-propanol or isopropanol. The results (Figure 4) demonstrate the concept of alcohol incorporation into one of the polymer units for each of these compounds. All fragments associated with methanol disappeared with incorporation of propanol (Table 2 and Figure 4). Note that for MEKP C3, an additional m/z 282.1911 peak was detected but presumed to be the in-source fragment of the major linear MEKP dihydroperoxy trimer (DHP3, $[M+NH_4]^+$ m/z 316.1966) since their XIC peak shapes matched (Figure 4). Furthermore, fragments other than m/z 95.0975 related to d_{18} -TATP

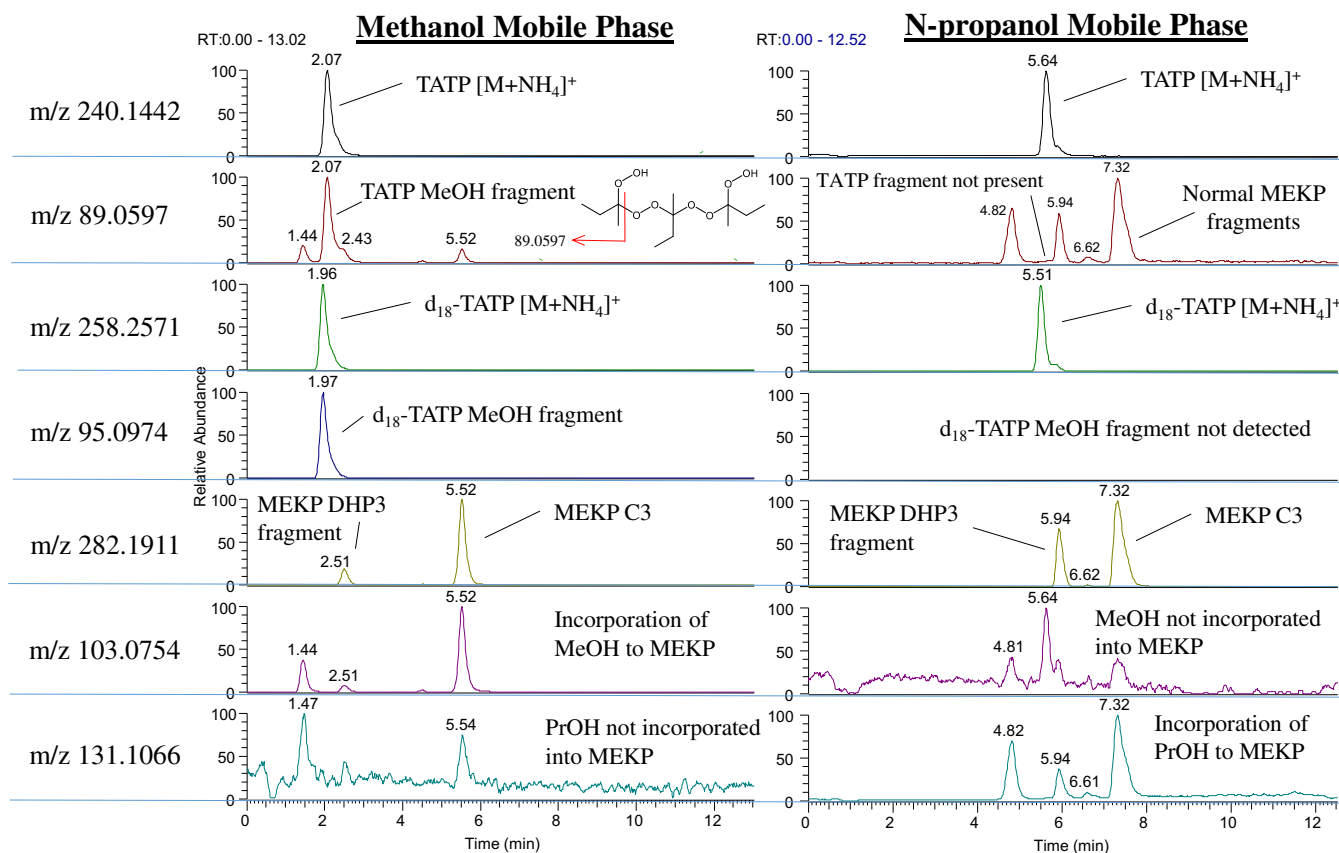


Figure 4. Chromatogram of mixture of TATP, d_{18} -TATP, and MEKP with mobile phase of MeOH or PrOH. Peak locations varied due to different chromatography conditions to accommodate the stronger solvent properties of PrOH versus MeOH. Multiple minor m/z 89 arise from normal fragments of MEKP

Table 2. Products ions associated with TATP and MEKP with and without incorporation of alcohols

TATP only							
Proposed Structure	Product	Material/solvent	Exact Mass	Molecular formula	Observed Mass	Δ PPM	Comments
	1	U/CH3OH	89.0597	C4H9O2+	89.0587	-11.2	Infusion experiment
		D18/CH3OH	95.0974	C4H3D6O2+	95.0964	-10.5	Infusion experiment
		U/CD3OD	92.0785	C4H6D3O2+	92.0776	-9.8	Infusion experiment
		U/PrOH	117.091	C6H13O2+	na	na	Contaminant present in solvent
		D18/PrOH	123.1287	C6H7D6O2+	123.1298	8.9	Observed in chromatogram
		U/CH3 ¹⁸ OH	91.0639	C4H9O ¹⁸ O+	91.0651	13.2	Infusion experiment
		D18/CH3 ¹⁸ OH	97.1016	C4H3D6O ¹⁸ O+	97.1027	11.3	Infusion experiment
	2	U/CH3OH	91.0390	C3H7O3+	91.038	-11.0	Infusion experiment
		D18/CH3OH	94.0578	C3H4D3O3+	94.0568	-10.6	Infusion experiment
		U/CD3OD	95.0641	C3H3D4O3+	95.0631	-10.5	Infusion experiment
		U/PrOH	119.0703	C5H11O3+	119.0715	10.1	Weak signal, Observed in chromatogram
		D18/PrOH	122.0891	C5H8D3O3+	122.0903	9.8	Weak signal, Observed in chromatogram
		U/CH3 ¹⁸ OH	93.0432	C3H7O2 ¹⁸ O+	93.0443	11.8	Infusion experiment
		D18/CH3 ¹⁸ OH	96.0620	C3H4D3O2 ¹⁸ O+	96.0632	12.5	Infusion experiment
	3	U/CH3OH	89.0597	C4H9O2+	89.0588	-10.1	Infusion experiment
		D18/CH3OH	92.0785	C4H6D3O2+	92.0776	-9.8	Infusion experiment
		U/CD3OD	95.0974	C4H3D6O2+	95.0964	-10.5	Infusion experiment
		U/PrOH	145.1223	C8H17O2+	145.1226	2.1	Observed in chromatogram
		D18/PrOH	148.1411	C8H14D3O2+	148.1415	2.7	Observed in chromatogram
		U/CH3 ¹⁸ OH	93.0682	C4H9 ¹⁸ O2+	93.0693	11.8	Infusion experiment
		D18/CH3 ¹⁸ OH	96.0870	C4H6D3 ¹⁸ O2+	96.0881	11.4	Infusion experiment
	4	U/CH3OH	91.0390	C3H7O3+	91.0380	-11.0	Infusion experiment
		D18/CH3OH	97.0766	C3HD6O3+	97.0757	-9.3	Infusion experiment
		U/CD3OD	92.0452	C3H6DO3+	92.0443	-9.8	Infusion experiment
		U/PrOH	na	na	na	na	No alcohol incorporated
		D18/PrOH	na	na	na	na	No alcohol incorporated
	5	U/CH3OH	75.0441	C3H7O2+	75.0431	-13.3	Infusion experiment
		D18/CH3OH	81.0817	C3HD6O2+	81.0808	-11.1	Infusion experiment
		U/CD3OD	76.0503	C3H6DO2+	76.0494	-11.8	Infusion experiment
		U/PrOH	na	na	na	na	No alcohol incorporated
		D18/PrOH	na	na	na	na	No alcohol incorporated
	6	U/CH3OH	74.0362	C3H6O2+	74.0353	-12.2	Infusion experiment
		D18/CH3OH	80.0739	C3D6O2+	80.0730	-11.2	Infusion experiment
		U/CD3OD	74.0362	C3H6O2+	74.0353	-12.2	Infusion experiment
		U/PrOH	na	na	na	na	No alcohol incorporated
		D18/PrOH	na	na	na	na	No alcohol incorporated
MEKP only (Deuterated material not available)							
Proposed Structure	Product	Material/solvent	Exact Mass	Molecular formula	Observed Mass	Δ PPM	Comments
	7	U/CH3OH	103.0754	C5H11O2+	103.0765	10.7	Not present when using PrOH
		U/PrOH	131.1067	C7H15O2+	131.1078	8.4	Not present when using MeOH
		U/CH3 ¹⁸ OH	105.0796	C5H11O ¹⁸ O+	105.0807	10.5	Infusion experiment
	8	U/CH3OH, R=Me	89.0597	C4H9O2+	89.0609	13.5	Also from MEKP fragment similar to Product E
		U/CH3OH, R=Et	103.0754	C5H11O2+	103.0765	10.7	May also be from Product G
		U/PrOH, R=Me	145.1223	C8H17O2+	145.1226	2.1	Observed in chromatogram
		U/PrOH, R=Et	159.13796	C9H19O2+	na	na	Contaminant present in solvent
		U/CH3 ¹⁸ OH, R=Me	93.0682	C4H9 ¹⁸ O2+	93.0693	11.8	Infusion experiment
		U/CH3 ¹⁸ OH, R=Et	107.0839	C5H11 ¹⁸ O2+	107.0849	9.3	Infusion experiment
	9	U/CH3OH	88.0519	C4H8O2+	88.0531	13.6	Cyclic Trimer only

U/CH3OH = Unlabeled material/Methanol solvent

D18/CH3OH = D18-Material/Methanol solvent

U/CD3OD = Unlabeled material/D-labeled solvent

U/PrOH = Unlabeled material/Propyl alcohol solvent

D18/PrOH = D18-Material/Propyl alcohol solvent

U/CH3¹⁸OH = Unlabeled material/¹⁸O-labeled MethanolD18/CH3¹⁸OH = D18-Material/¹⁸O-labeled Methanol

Red structural components suggest incorporation of solvent alcohol

MeOH incorporation were consistently observed at m/z 97.0766 ($C_3H_6D_3O_3^+$) and m/z 92.0785 ($C_4H_6D_3O_2^+$). To probe these findings, complete HDX experiments were performed on TATP

and d_{18} -TATP. Multiple fragments were observed (Table 2). Figure 5 shows the full scan spectra (from $\sim m/z$ 50 to 120 for resolution purposes) of the infusion of d_{18} -TATP and TATP with

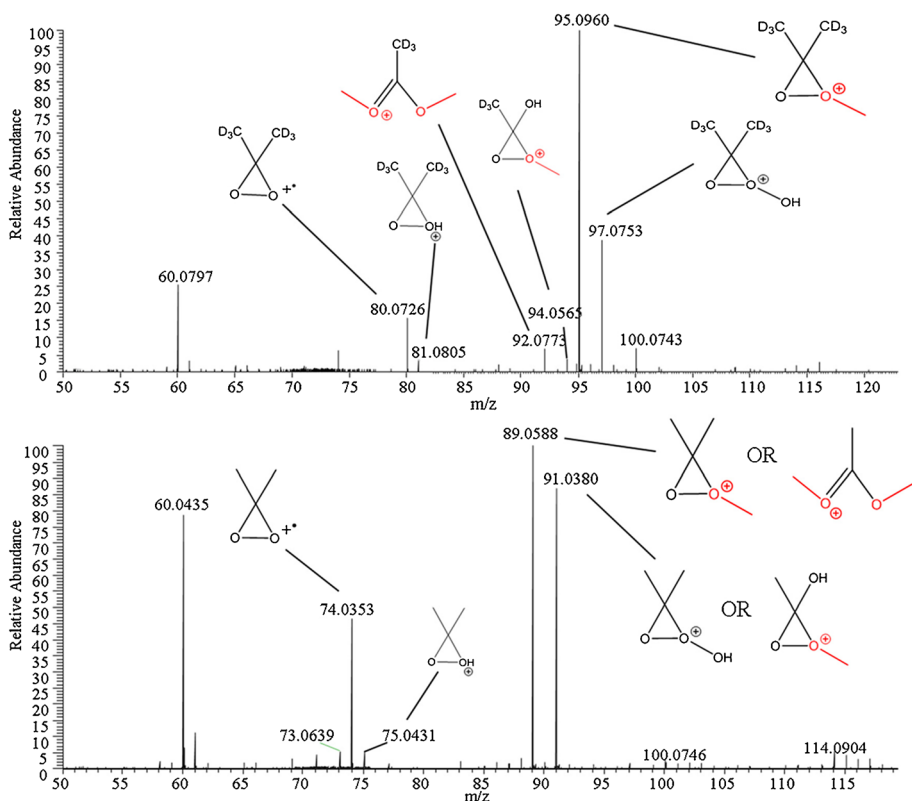


Figure 5. MP infusion of d_{18} -TATP (top) and TATP (bottom) in CH_3OH showing low mass range and proposed in-source fragment assignments. Incorporated solvent MeOH molecules are red

the proposed in-source fragment assignments. The fragment m/z 92.0785 corresponds to the incorporation of 2 alcohol. Importantly, for non-deuterated TATP, this peak is also m/z 89.0975. This is critical since every molecule of TATP present may react with either one or two molecules of alcohol depending on the conditions of the method. Slight variations in the method generally result in vastly different results when monitoring any of these low mass fragments, particularly m/z 89.

To test the conditions that contribute to fragment formation, 20 $\mu\text{g}/\text{mL}$ of the d_{18} -TATP (90% MeOH/10% 10 mM NH_4OAc) was infused post column at 20 $\mu\text{L}/\text{min}$ into 230 $\mu\text{L}/\text{min}$ of LC flow (90% MeOH/10% 10 mM NH_4OAc —high concentration to ensure observation). The m/z values of 258, 97, 95, and 92 correspond to the parent d_{18} -TATP and products **4**, **1**, and **3**, (Table 2), respectively. At a vaporizer temperature of 250 $^\circ\text{C}$, the signal for all ions seemed to be

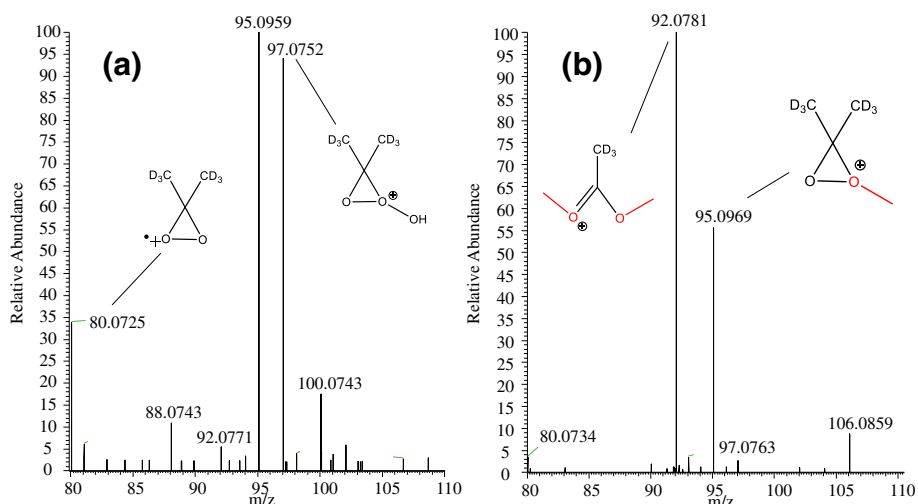
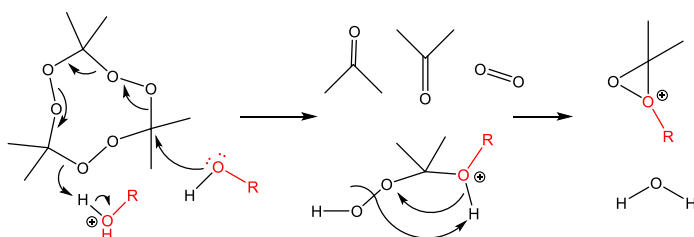


Figure 6. APCI source data from (a) direct infusion of 20 $\mu\text{L}/\text{min}$ d_{18} -TATP versus (b) 20 $\mu\text{L}/\text{min}$ d_{18} -TATP infused into a mobile phase containing 90% MeOH/10% 10 mM NH_4OAc at 230 L/min



Scheme 1. Proposed mechanism for the addition of one alcohol to TATP

Alcohol	R	m/z Expected	m/z Observed	Δ PPM
Methanol	-CH ₃	89.0597	89.0605	8.98
Ethanol	-CH ₂ CH ₃	103.0754	103.0768	13.58
Propanol	-(CH ₂) ₂ CH ₃	117.0910	N/A	
Butanol	-(CH ₂) ₃ CH ₃	131.1067	131.1080	9.92
tert-Butanol	-C(CH ₃) ₃	131.1067	131.1079	9.15

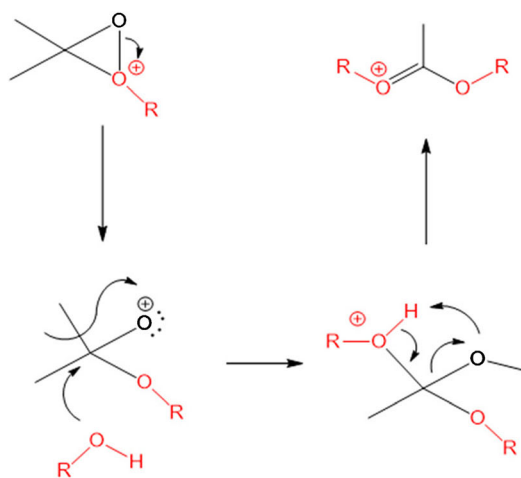
optimized, with **3** being the most intense ion followed closely by **1**. As gas flow from the auxiliary/sheath gas was increased, **1** began to dominate over **3** with little change in either parent or **4** (which was only marginally detected). However, when the LC flow was removed and the same d_{18} -TATP solution was directly infused at 20 μ L/min into the high gas flow at 250 $^{\circ}$ C, product **4** became the most intense ion with nearly the same intensity as the parent. As gas flow was pushed even higher, parent and product **4** were nearly all that could be seen, with no **3** present at all. As gas flow was dropped to minimal values (sheath 8 AU and aux 5 AU), product **1** dominated the spectrum, and **3** became slightly more intense than **4**, which had dropped significantly. This suggests that at higher gas flows, ions are pushed into the MS more rapidly with either less time in the corona region or less time exposed to the vaporizer temperature to react with the solvent to form alcohol-incorporated products. Additionally, when infused into the mobile phase (versus direct infusion) that contains a significantly higher population of MeOH ions/molecules, far more of the alcohol incorporated products are observed (Figure 6).

To be sure that the incorporation of the alcohol is completed, a study with the infusion of TATP, d_{18} -TATP, and MEKP in Me¹⁸OH was performed. Complete incorporation of both the carbon and the oxygen from MeOH into each of the proposed products was observed (Figure S-2., [Online Resource](#)). For this analysis, source conditions that favored the formation of the alcohol incorporated products were used. Owing to the cost of

the ¹⁸O solvents, we were unable to attempt this at mobile phase levels; therefore, doubly incorporated products at m/z 93.0693 and 96.0881 were not as significant as shown in Figure 6b. Scheme 1 shows the proposed mechanism for the formation of Product **1**, Table 2. Note that an interfering component at m/z 117.0920 was present in either PrOH or IPA that obscured detection of the PrOH-TATP product.

Scheme 2 shows the proposed mechanism for the addition of the second alcohol from the product of Scheme 1. With the abundance of this fragment (depending on conditions used) it may transform by a more concerted mechanism than proposed. It should be noted that as the alcohol chain length increased, the addition of two alcohols seemed to become more significant than the addition of one alcohol. Also, formation of the tert-BuOH product for either one or two additions of alcohol was nearly non-existent. This supports the proposed mechanisms since steric interactions would prevent this reaction.

Cyclic peroxides appear to have several analytical nuances that separate them from their linear counterparts. The structure of TATP has, of course, been confirmed by X-ray diffraction and other spectroscopic techniques with subsequent DFT calculations to corroborate this data [5, 39, 40]. However, there has been no definitive identification of the cyclic MEKP species. MEKP product **9** (m/z 88.0519) in Table 2 was only produced by the presumed cyclic MEKP C3 trimer. Because TATP also forms this analog (product **6**, Table 2) this suggests that the species we are calling



Scheme 2. Proposed mechanism for the addition of a second alcohol to TATP

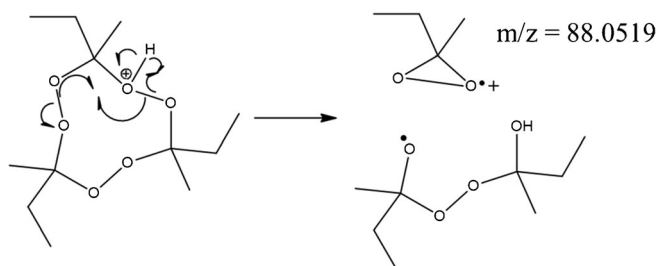
Alcohol	R	m/z Expected	m/z Observed	Δ PPM
Methanol	-CH ₃	89.0597	89.0605	8.98
Ethanol	-CH ₂ CH ₃	117.091	117.0924	11.96
Propanol	-(CH ₂) ₂ CH ₃	145.1223	145.1228	3.45
Butanol	-(CH ₂) ₃ CH ₃	173.1536	173.1541	2.89
tert-Butanol	-C(CH ₃) ₃	173.1536	173.1542	3.47

MEKP C3 is indeed the cyclic trimer. No other observed MEKP species (all presumably linear) formed product **9**, suggesting that the *cis* configuration of the cyclic species is required to form this product. The mechanism is proposed in Scheme 3. It is also notable that while the linear MEKP ionized quite well by electrospray ionization (ESI), the cyclic peroxides (TATP, MEKP C3, and HMTD) prefer APCI. Attempts to isolate MEKP on the CombiFlash system using a C18 column gave inconclusive results for collection of the cyclic trimer utilizing the ESI source for MS collection triggering. When the APCI source was applied, a strong signal at nominal mass m/z 282 dominated the spectrum. This suggests that the structure of this compound is fundamentally different from other components in the MEKP mixture and is most likely cyclic in nature.

Attempts to Enhance Signal Intensity

Although the sodium adduct of TATP has been used by Desorption ESI (DESI) [26], Extractive ESI (EESI) [24], and LC-ESI [23] to produce abundant ions at m/z 245.0996, our attempts at adding controlled amounts of very low concentrations of sodium to the mobile phase for quantitative analysis ended with plugged electrospray capillaries. However, even using sodium, we have been unable to approach the level of quantification provided by APCI for TATP (currently, 1 ng on column for m/z 240.1442 and 200 pg on column for m/z 89.0597). TATP (and all the peroxides associated with MEKP) have historically been observed only as ammonium or sodium adducts in our lab. While in ESI, the TATP sodium adduct is rather intense, the addition of lithium and potassium did not produce a significant signal compared with either sodium or ammonium, suggesting the size of these ions is optimal for gas-phase adduction.

As mentioned above, variation in gas flow affected the intensity and abundance of each ion associated with TATP. To optimized APCI conditions for either the TATP $[M+NH_4]^+$ or the m/z 89 signal, injections ($N = 3$) were made on the C18 column at various conditions of temperature, gas flow, and mobile phase modifier (the LC flow was kept at 250 μ L/min). At a vaporizer temperature of 250 $^{\circ}$ C, gas flows ranged from (sheath/aux 1:1) 30 to 70 AU with the most intense $[M+NH_4]^+$ at 70 AU and for m/z 89, 30 AU (nearly 1:1 signal for the d_{18} -TATP m/z 95:92 fragments). Temperature was then varied from 210 to 450 $^{\circ}$ C with the gas flow set to 30 AU. At



Scheme 3. Proposed mechanism for the formation of m/z 88 radical cation from MEKP C3

210 $^{\circ}$ C, TATP $[M+NH_4]^+$ was the most intense signal with the m/z 89 peak optimized at 300 $^{\circ}$ C (nearly 2.5:1 signal for the d_{18} -TATP m/z 95:92 fragments). Temperatures higher than this began to dramatically reduce the total signal. Removal of the ammonium source (mobile phase of water/MeOH) came with the expected reduction of the $[M+NH_4]^+$ signal (less than 1% of the total TATP signal). Surprisingly, the signal for the m/z 89 peak increased nearly 40% over the optimized conditions using 10 mM NH_4OAc (m/z 95 was 70% of the total signal and m/z 92 was 30% for the d_{18} -TATP sample). Based on this work, we have developed two methods for preferential detection of m/z 89 or m/z 240 for TATP. For the analysis of intact TATP or related compounds, we use the method optimized for $[M+NH_4]^+$ where the mobile phase has 10 mM NH_4OAc and MS conditions favoring m/z 240 production. For low level quantification, we use the method favoring the m/z 89 fragment with the aqueous mobile phase containing only 200 μ M NH_4OAc (a concentration that is comparable to no ammonium addition). Since the mobile phase flow rate would likely alter these conditions, and minor changes seem to correspond to significant ionization variability, each LC/MS instrument being used for the detection of peroxide explosives should be optimized for gas flow and temperature in addition to the instrument automatic signal optimization procedure.

In our lab, DADP has not been observed as the adduct of hydrogen (m/z 149.0808), ammonium (m/z 166.1074), sodium (m/z 171.0628), or lithium (m/z 155.0890) at reasonable levels (<500 μ M) for LC/MS analysis in ESI or APCI. At the level of 100 μ g/mL (675 μ M), m/z 166.1074 did begin to appear above the background noise. It is important to know that low concentrations of DADP can be observed as the alcohol incorporated fragment at m/z 89.0597 using APCI. On the LC system described above for TATP analysis, DADP elutes about 40 s earlier than TATP. Using the d_{18} -TATP as an IS, a dynamic range for DADP analysis was established between 20,000 and 100 ng/mL with a LOD of 50 ng/mL. Inadequate separation of TATP from other peroxides could provide significantly skewed results.

Conclusions

Two cautionary notes come from this research. First, while researchers have long been aware that TATP has a rather high vapor pressure for a solid, the fact that it readily volatilizes from solution has not been fully appreciated. Second, while low-levels of TATP may be quantified by LC/MS using the molecular fragment m/z 89, it must be recognized that this fragment has conditions. It represents two different species that are both dependent on the MeOH concentration, mobile phase modifiers, temperature, gas flow, and flow rate (among the parameters tested). Since the two most common LC/MS solvents for reverse phase chromatography are methanol and acetonitrile, the analyst is faced with a dilemma. If acetonitrile is used as the mobile phase, ionization is suppressed below reasonable levels of analytical detection [35]. If methanol is used, the compound

will invariably react with the species in the gas phase. The gas-phase alcohol attack of peroxides (TATP, DADP, MEKP, and HMTD) at the α -carbon is apparently a general phenomenon [14, 38]. This phenomenon can be exploited to lower the limits of detection for these compounds. However, understanding the origins of a particular fragment is very important, and all variables must be considered prior to using these ions for quantification. Proper separation must be achieved to prevent unwanted materials (many small compounds may have a mass associated with $C_4H_9O_2^+$) from providing a false positive response. Also, analytical conditions may significantly affect this particular signal response, making it more susceptible to interference from unknown co-eluting ion suppressors or enhancers. Lastly, other factors outside the scope of this research may influence the formation of peroxide products [41].

Acknowledgments

This material is based upon work supported by US Department of Homeland Security (DHS), Science and Technology Directorate, Office of University Programs, under Grant 2013-ST-061-ED0001. Views and conclusions are those of the authors and should not be interpreted as necessarily representing the official policies, either expressed or implied, of DHS.

References

1. Wolffenstein, R.: [Ueber die Einwirkung von Wasserstoffsperoxyd auf Aceton und Mesityloxyd.] *Chem. Berlin* **28**, 2265–2269 (1895)
2. Legler, L.: [Ueber die sogenannte Aether- oder Lampenaiiare.] *Chem. Berlin* **14**, 602–604 (1881)
3. Milas, N.A., Golubovic, A.: Studies in organic peroxides. XXV. Preparation, separation and identification of peroxides derived from methyl ethyl ketone and hydrogen peroxide. *J. Am. Chem. Soc.* **81**, 5824–5826 (1959)
4. Oxley, J., Smith, J., Brady, J., Dubnikova, F., Kosloff, R., Zeiri, L., Zeiri, Y.: Raman and infrared fingerprint spectroscopy of peroxide-based explosives. *Appl. Spectrosc.* **62**, 906–915 (2008)
5. Jensen, L., Mortensen, P.M., Trane, R., Harris, P., Berg, R.W.: Reaction kinetics of acetone peroxide formation and structure investigations using Raman spectroscopy and X-ray diffraction. *Appl. Spectrosc.* **63**, 92–97 (2009)
6. Kozole, J., Tomlinson-Phillips, J., Stairs, J.R., Harper, J.D., Lukow, S.R., Lareau, R.T., Boudries, H., Lai, H., Brauer, C.S.: Characterizing the gas phase ion chemistry of an ion trap mobility spectrometry based explosive trace detector using a tandem mass spectrometer. *Talanta* **99**, 799–810 (2012)
7. Tomlinson-Phillips, J., Wooten, A., Kozole, J., Deline, J., Beresford, P., Stairs, J.: Characterization of TATP gas phase product ion chemistry via isotope labeling experiments using ion mobility spectrometry interfaced with a triple quadrupole mass spectrometer. *Talanta* **127**, 152–162 (2014)
8. Jiang, D., Peng, L., Wen, M., Zhou, Q., Chen, C., Wang, X., Chen, W., Li, H.: Dopant-assisted positive photoionization ion mobility spectrometry coupled with time-resolved thermal desorption for on-site detection of triacetone triperoxide and hexamethylene trioxide diamine in complex matrices. *Anal. Chem.* **88**, 4391–4399 (2016)
9. Bauer, C., Willer, U., Lewicki, R., Pohlkötter, A., Kosterev, A., Kosynkin, D., Tittel, F.K., Schade, W.: A mid-infrared QEPAS sensor device for TATP detection. *J. Phys. Conf. Ser.* **157**, 1–6 (2009)
10. Hildenbrand, J., Herbst, J., Wöllenstein, J., Lambrecht, A.: Explosive detection using infrared laser spectroscopy. *Proc. SPIE Int. Soc. Opt. Eng.* **7222**, 72220B1–72220B-12 (2009)
11. Armit, D., Zimmermann, P., Ellis-Steinborner, S.: Gas chromatography/mass spectrometry analysis of triacetone triperoxide (TATP) degradation products. *Rapid Commun. Mass Spectrom.* **22**, 950958 (2008)
12. Romolo, F.S., Cassioli, L., Grossi, S., Cinelli, G., Russo, M.V.: Surface-sampling and analysis of TATP by swabbing and gas chromatography/mass spectrometry. *Forensic Sci. Int.* **224**, 96–100 (2013)
13. Oxley, J.C., Smith, J.L., Bowden, P.R., Rettinger, R.C.: Factors influencing triacetone triperoxide (TATP) and diacetone diperoxide (DADP) formation: Part 1. *Propellants Explos. Pyrotech.* **38**, 244–254 (2013)
14. Rondeau, D., Vogel, R., Tabet, J.-C.: Unusual atmospheric pressure chemical ionization conditions for detection of organic peroxides. *Sect. Title Org. Anal. Chem.* **38**, 931–940 (2003)
15. Oxley, J., Zhang, J., Smith, J., Cioffi, E.: Mass spectra of unlabeled and isotopically labeled hexamethylene triperoxide diamine (HMTD). *Propellants Explos. Pyrotech.* **25**, 284–287 (2000)
16. Oxley, J., Smith, J., Shinde, K., Moran, J.: Determination of the vapor density of triacetone triperoxide (TATP) using a gas chromatography headspace technique. *Propellants Explos. Pyrotech.* **30**, 127–130 (2005)
17. Evans, H.K., Tulleners, F.A.J., Sanchez, B.L., Rasmussen, C.A.: An unusual explosive, triacetone triperoxide (TATP). *J. Forensic Sci.* **31**, 1119–1125 (1986)
18. Sigman, M.E., Clark, C.D., Fidler, R., Geiger, C.L., Clausen, C.A.: Analysis of triacetone triperoxide by gas chromatography/mass spectrometry and gas chromatography/tandem mass spectrometry by electron and chemical ionization. *Rapid Commun. Mass Spectrom.* **20**, 2851–2857 (2006)
19. Burks, R.M., Hage, D.S.: Current trends in the detection of peroxide-based explosives. *Anal. Bioanal. Chem.* **395**, 301–313 (2009)
20. Peña-Quevedo, A.J., Hernández-Rivera, S.P.: Mass spectrometry analysis of hexamethylene triperoxide diamine by its decomposition products. *Proc. SPIE Int. Soc. Opt. Eng.* **7303**, 730303-1–730303-11 (2009)
21. Widmer, L., Watson, S., Schlatter, K., Crowson, A.: Development of an LC/MS method for the trace analysis of triacetone triperoxide (TATP). *Analyst* **127**, 1627–1632 (2002)
22. Cotte-Rodríguez, I., Chen, H., Cooks, R.G.: Rapid trace detection of triacetone triperoxide (TATP) by complexation reactions during desorption electrospray ionization. *Chem. Commun.* 953–955 (2006)
23. Sigman, M.E., Clark, C.D., Caiano, T., Mullen, R.: Analysis of triacetone triperoxide (TATP) and TATP synthetic intermediates by electrospray ionization mass spectrometry. *Rapid Commun. Mass Spectrom.* **22**, 84–90 (2008)
24. Hill, A.R., Edgar, M., Chatzigeorgiou, M., Reynolds, J.C., Kelly, P.F., Creaser, C.S.: Analysis of triacetone triperoxide complexes with alkali metal ions by electrospray and extractive electrospray ionisation combined with ion mobility spectrometry and mass spectrometry. *Eur. J. Mass Spectrom.* **21**, 265–274 (2015)
25. Hagenhoff, S., Franzke, J., Hayen, H.: Determination of peroxide explosive TATP and related compounds by dielectric barrier discharge ionization-mass spectrometry (DBDI-MS). *Anal. Chem.* **89**, 4210–4215 (2017)
26. Cotte-Rodríguez, I., Hernández-Soto, H., Chen, H., Cooks, R.G.: In situ trace detection of peroxide explosives by desorption electrospray ionization and desorption atmospheric pressure chemical ionization. *Anal. Chem.* **80**, 1512–1519 (2008)
27. Xu, X., van de Craats, A.M., Kok, E.M., de Bruyn, P.C.A.M.: Trace analysis of peroxide explosives by high performance liquid chromatography-atmospheric pressure chemical ionization-tandem mass spectrometry (HPLC-APCI-MS/MS) for forensic applications. *J. Forensic Sci.* **49**, 1–7 (2004)
28. Xu, X., Koeberg, M., Kuijpers, C.-J., Kok, E.: Development and validation of highly selective screening and confirmatory methods for the qualitative forensic analysis of organic explosive compounds with high performance liquid chromatography coupled with (photodiode array and) LTQ ion trap/Orbitrap. *Sci. Justice* **54**, 3–21 (2014)
29. Rapp-Wright, H., McEneff, G., Murphy, B., Gamble, S., Morgan, R., Beardah, M., Barron, L.: Suspect screening and quantification of trace organic explosives in wastewater using solid phase extraction and liquid chromatography-high resolution accurate mass spectrometry. *J. Hazard. Mater.* **329**, 11–21 (2017)
30. DeTata, D., Collins, P., McKinley, A.: A fast liquid chromatography quadrupole time-of-flight mass spectrometry (LC-QToF-MS) method for the identification of organic explosives and propellants. *Forensic Sci. Int.* **233**, 63–74 (2013)

31. Krawczyk, T.: Enhanced electrospray ionization mass spectrometric detection of hexamethylene triperoxide diamine (HMTD) after oxidation to tetramethylene diperoxide diamine dialdehyde (TMDDD). *Rapid Commun. Mass Spectrom.* **29**, 2257–2262 (2015)
32. Marsh, C.M., Mothershead, R.F., Miller, M.L.: Post-blast analysis of hexamethylene triperoxide diamine using liquid chromatography-atmospheric pressure chemical ionization-mass spectrometry. *Sci. Justice.* **55**, 299–306 (2015)
33. Newsome, G.A., Ackerman, L.K., Johnson, K.J.: Humidity affects relative ion abundance in direct analysis in real time mass spectrometry of hexamethylene triperoxide diamine. *Anal. Chem.* **86**, 11977–11983 (2014)
34. Crowson, A., Beardah, M.S.: Development of an LC/MS method for the trace analysis of HMTD. *Analyst.* **126**, 1689–1693 (2001)
35. Colizza, K., Mahoney, K.E., Yevdokimov, A.V., Smith, J.L., Oxley, J.C.: Acetonitrile ion suppression in atmospheric pressure ionization mass spectrometry. *J. Am. Soc. Mass Spectrom.* **27**, 1796–1804 (2016)
36. Wierzbicki, A., Salter, E.A., Cioffi, E.A., Stevens, E.D.: Density functional theory and X-ray investigations of P- and M-hexamethylene triperoxide diamine and its dialdehyde derivative. *J. Phys. Chem. A.* **105**, 8763–8768 (2001)
37. Smith, M.E., Wall, C., Fitzgerald, M.: Characterization of the major synthetic products of the reactions between butanone and hydrogen peroxide. *Propellants Explos. Pyrotech.* **37**, 282–287 (2012)
38. Colizza, K., Porter, M., Smith, J.L., Oxley, J.C.: Gas-phase reactions of alcohols with hexamethylene triperoxide diamine (HMTD) under atmospheric pressure chemical ionization conditions. *Rapid Commun. Mass Spectrom.* **29**, 74–80 (2014)
39. Groth, P.: Crystal structure of 3,3,6,6,9,9-hexamethyl-1,2,4,5,7,8-hexaoxacyclononane (“trimeric acetone peroxide”). *Acta Chem. Scand.* **23**, 1311–1329 (1969)
40. Dubnikova, F., Kosloff, R., Almog, J., Zeiri, Y., Boese, R., Itzhaky, H., Alt, A., Keinan, E.: Decomposition of triacetone triperoxide is an entropic explosion. *J. Am. Chem. Soc.* **127**, 1146–1159 (2005)
41. Newsome, G.A., Ackerman, L.K., Johnson, K.J.: Humidity effects on fragmentation in plasma-based ambient ionization sources. *J. Am. Soc. Mass Spectrom.* **27**, 135–143 (2016)